Rock Mech. Rock Engng. (1995) 28 (4), 211–226

Rock Mechanics and Rock Engineering

The Application of Energy Principles to the Determination of the Sliding Resistance of Rock Joints

By

J. P. Seidel and **C. M. Haberfield**

Monash University, Clayton, Australia

Summary

Energy principles have previously been applied to the analysis of rock joints in order to determine the shear strength of dilatant joints (Ladanyi and Archambault, 1970). This work was based on the analysis of regular triangular asperities and assumed that the asperities were rigid. In recognition of the difficulty of measuring a representative asperity angle in natural, complex rock joints, Ladanyi and Archambault extended their results to natural joints by assuming the equality of joint dilation rate and the effective joint asperity angle. It is shown that the assumption of this equality is not universally valid, and that it may lead to an underestimation of joint shear strength. Further, the effective friction angle for joints in an elastic rock mass, for joints comprising asperities of varying inclination, for post-peak shear displacements and for joints in degradable rock are all analysed using extensions of Ladanyi and Archambault's approach.

1. Introduction

The shear strength of rock joints is derived in part from the basic sliding friction angle of the parent rock (in the absence of any joint weathering or cementing) and in part by the roughness of the joint, which causes the joint to dilate as shear displacement proceeds. This dilational component of shear strength has been incorporated in many joint shear models. Patton (1966) performed a series of constant normal load direct shear tests on sawtooth-shape plaster/kaolin asperities of uniform inclination, i, at varying normal stresses. From these tests, he established a bilinear failure envelope with a transition pressure defining the change of failure from an asperity sliding to an asperity shearing mode.

As shown in Fig. 1, the failure envelope comprises two linear sections, intersecting at a normal stress, σ_T, designated the transition stress. For normal stresses, σ_n, less than σ_T, the peak shear stress, τ_p, is governed by sliding at the sliding friction angle, ϕ_μ, and the asperity inclination, i. Above this transition stress, the peak shear stress is governed by shearing through the asperities with a shear strength intercept, c_j, and a residual angle of internal friction, ϕ_r. The

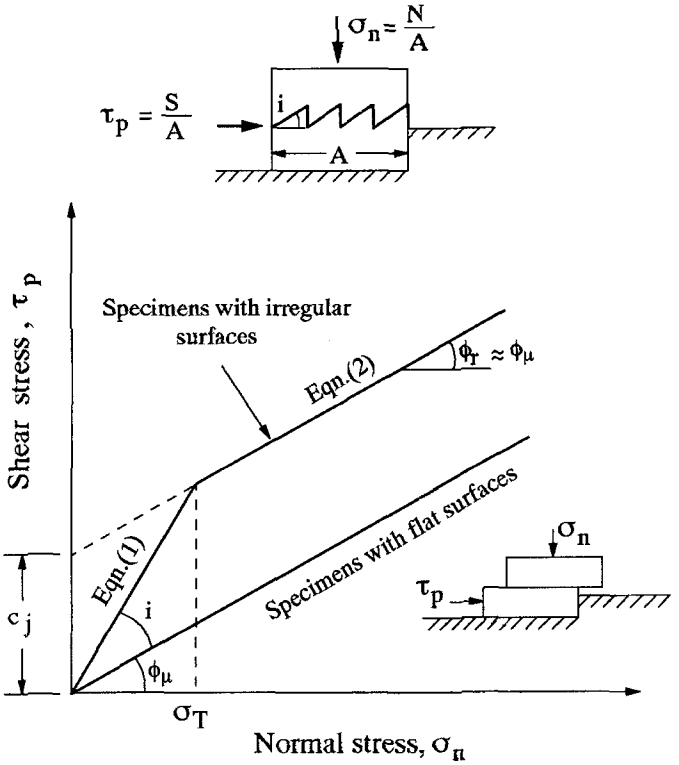

Fig. 1. Patton's bilinear failure model (after Patton, 1966)

equations for the two portions of the failure envelope are given below:

$$\tau_p = \sigma_n \tan(\phi_\mu + i) \quad \text{for } \sigma_n < \sigma_T \tag{1}$$

$$\tau_p = c_j + \sigma_n \tan \phi_r \quad \text{for } \sigma_n \geq \sigma_T \tag{2}$$

$$\text{where } \sigma_T = \frac{c_j}{\tan(\phi_u + i) - \tan \phi_r}. \tag{3}$$

The important feature of this early model is that it captured two basic mechanisms of behaviour of rock joints, namely: asperity sliding and asperity shearing. Patton showed that the effect of uniform asperities at a uniform angle, i, with the mean sliding surface is to increase the friction angle by i, with an associated dilatancy, $\psi = |x \tan i|$, where x is the shear displacement, and the absolute value signifies positive dilation for shear in opposite directions. The curvilinear failure envelopes of natural rock joints was attributed to the change in intensities of the different modes of failure occurring simultaneously.

Ladanyi and Archambault (1970) provided an extension to Patton's joint model to account for the sliding and shearing mechanisms found in natural rock joints. They considered the shear resistance of joints comprising regular triangular asperities with asperity angles of $\pm i°$. However, instead of adopting the force equilibrium approach used by Patton, they used the energy principles described by Rowe (1962) and Rowe et al. (1964).

According to Ladanyi and Archambault, the total shearing force, S, can be considered as the sum of 4 components, 1 of which (S_4) relates to force attributed to asperity shearing, and 3 of which (S_1 to S_3) relate to the process of asperity sliding. Hence they determined the sliding shear force as:

$$S = S_1 + S_2 + S_3, \tag{4}$$

where,

S_1 = component due to external work done in dilating against the normal force $(N) = N\dot{\nu}$, where $\dot{\nu}$ is the rate of dilation at failure.

S_2 = component due to the additional internal work in friction due to dilatancy = $S\dot{\nu} \tan \phi_\mu$, where ϕ_μ is the basic angle of frictional sliding resistance.

S_3 = component due to work done in internal friction if sample did not change in volume in shear = $N \tan \phi_\mu$.

Recognizing that in an irregular surface both sliding and shearing mechanisms would exist simultaneously, and defining the projected area of the shearing asperities at the point of failure, A_S, Ladanyi and Archambault then defined the total shear force, S, as

$$S = (S_1 + S_2 + S_3)\ (1 - a_S) + S_4\ a_S, \tag{5}$$

where,

S_4 = component due to shearing through rock asperities at the base = $A\, s_0 + N \tan \phi_0$ where A is the total projected joint area, and s_0 and ϕ_0 are the intact rock strength parameters, and

a_s = the shear area ratio, and defines the relative area of joint undergoing shearing = A_S/A.

As the authors are concerned here only with sliding mechanisms of failure, further discussion will be restricted to three sliding components (S_1 to S_3). These components are shown diagrammatically in Fig. 2.

The dilation rate at failure, $\dot{\nu}$ is equal to the ratio of the increments of dilation, dy, and shear displacement, dx. The ratio dy/dx can therefore be substituted for $\dot{\nu}$ in each of the foregoing expressions for the components S_1, S_2 and S_3, and

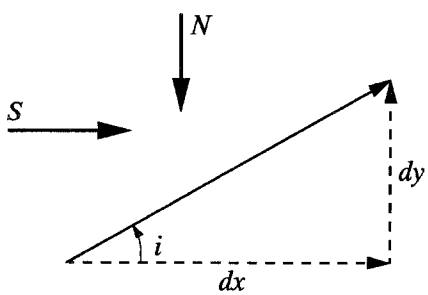

$$S_1 = \frac{N\,dy}{dx} = N \tan i$$

$$S_2 = S \tan i \tan \phi_u$$

$$S_3 = N \tan \phi_u$$

$$S = S_1 + S_2 + S_3$$

Fig. 2. Ladanyi and Archambault's (1970) frictional work components

substituted into Eq. (4) as follows:

$$S = N\frac{dy}{dx} + S\tan\phi_u\frac{dy}{dx} + N\tan\phi_u \tag{6}$$

As the analysis by Ladanyi and Archambault is based on the assumption of a rigid asperity, the dilation rate, dy/dx, is also equal to the tangent of the asperity angle, i. Equation (6) can therefore be rearranged, and converted to stress units to give:

$$\tau = \frac{\sigma_n(\tan i + \tan\phi_u)}{(1 - \tan\phi_u \tan i)} \tag{7}$$

which can be simplified to the following expression derived by Ladanyi and Archambault:

$$\tau = \sigma_n \tan(\phi_u + i) \tag{8}$$

Equation (8) is identical to that obtained by Patton for the peak sliding resistance of sawtooth profiles with inclination, i, at normal stress levels less than the transition pressure.

Ladanyi and Archambault suggest that for irregular surfaces, which exhibit complex geometry (rather than trivial first-order roughness as exemplified by the simple triangular model), the asperity angle, i, cannot be determined, and the dilation rate, $\dot{\nu}$, should be substituted. Furthermore, they recommend that ϕ_u should be more correctly replaced by the empirically determined statistical average value of friction angle, ϕ_f. On the basis of investigations by Rowe (1962), they tentatively determine for initially tightly interlocked rock surfaces, such as are being considered here, that ϕ_f would not be much different from ϕ_u. Hence in its simplest and most basic form, and ignoring the shearing component, Ladanyi and Archambault recommend for the sliding resistance of natural rock joints with their attendant complex joint geometry:

$$\tau = \frac{\sigma_n(\dot{\nu} + \tan\phi_u)}{1 - \dot{\nu}\tan\phi_u} \tag{9}$$

or,

$$\tau = \sigma_n \tan(\phi_u + \nu), \text{where } \nu = \tan^{-1}[\dot{\nu}]. \tag{10}$$

It is noted that Eqs. (9) and (10) relate only to the sliding component of friction. The further complexities of the shearing component and interlocking factors also derived by Ladanyi and Archambault are peripheral to the purpose of this paper, and only the basic sliding shear stress component as reflected in Eq. (10) will be considered hereafter.

2. Energy Approach for Elastic Materials

The validity of Eq. (10) for the rigid asperities assumed by Ladanyi and Archambault can be easily verified by considering a profile with only first order roughness, such as simple triangular asperities. As the dilation angle and asperity

angle are identical, if Eq. (8) is correct, then Eq. (10) must follow. However, it will be readily appreciated that for interfaces comprising elastic materials, elastic deformations will result in joint dilation rates less than the asperity angle, and that the values of asperity angle and dilation rate are not interchangeable in these circumstances.

The energy approach outlined previously can be successfully extended from rigid to elastic asperities. Rigid asperities do not, by definition, undergo any deformation due to the applied shear and normal loads. However, for elastic materials, the elastic, and recoverable, deformations must be taken into account. The following analysis will be restricted to a consideration of deformations perpendicular to the joint axis only, however, the same considerations apply to the treatment of elastic shear deformations. Figure 3 shows a deformation due to

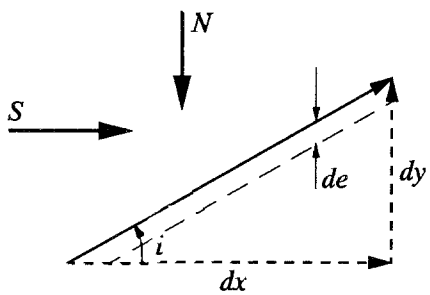

$$S_1 = \frac{N(dy\text{-}de)}{dx} + \frac{Nde}{dx} = N \tan i$$

$$S_2 = S \tan i \tan \phi_u$$

$$S_3 = N \tan \phi_u$$

$$S = S_1 + S_2 + S_3$$

Fig. 3. Deformations due to elasticity

elasticity in the vertical direction, *de*, during the sliding process. This deformation effectively causes a vertical body motion of the interface by the amount *de*, and a reduction in the joint dilation to *dy-de*.

The *relative* movements between opposing surfaces on the interface, however, remain unchanged – that is: the movements resulting in frictional losses remain *dx* in the x-direction, and *dy* in the y-direction. Therefore, following the terminology used by Ladanyi and Archambault in their energy approach, force components S_2 and S_3 are identical to the original rigid asperity case.

By contrast, component S_1 is reduced, in as much as dilation is reduced from *dy* to (*dy-de*). However, as the deformations are elastic and recoverable, the reduction in work done in dilating against the external normal force is exactly balanced by additional work required to increase the internal strain energy of the asperities, *dU*, i.e.

$$dU = N.de \tag{11}$$

The net effect on the component S_1 is consequently nil. Therefore, although the effect of elasticity is to reduce the net dilation rate as a result of asperity deformation from $dy/dx = \tan i$ to $(dy\text{-}de)/dx < \tan i$, the frictional resistance is unchanged, i.e.

$$\tau = \sigma_n \tan(\phi_u + i). \tag{12}$$

Equation (12) has been verified experimentally by Seidel (1993) for a series of constant normal stiffness direct shear tests on regular triangular joint profiles cut into a synthetic mudstone material, called Johnstone (1986). These tests were performed as part of an extensive research project into the behaviour of concrete piles socketed into weak rock; the joint in these tests therefore comprised a weak rock/concrete interface. Asperity angles for these tests varied from 5° to 27.5°, and typical interface geometry, shear displacement-dilation curves and stress-path plots are shown for tests on regular triangular asperities of 12.5° and 22.5° in Fig. 4 and Fig. 5 respectively.

The effective friction angle predicted by Eq. (12) for the series of tests, $(\phi_u + i)$, is compared in Table 1 with both $\tan^{-1}(\tau/\sigma_n)$ measured in the tests and the effective friction angle, $(\phi_u + \nu)$, suggested by Eq. (10). It is clear from this table that the joint dilation angle is consistently lower than the asperity angle, and that the observed joint sliding friction angle $[\tan^{-1}(\tau/\sigma_n)]$ is by far more closely predicted by Eq. (12) than Eq. (10). The boundary conditions adopted in these tests were approximately 300 kPa initial normal stress and a constant normal stiffness of 300 kPa/mm dilation, except for the test on the 5° sample, for which double these values were used. For regular triangular asperities, Eq. (10) underestimates the joint shear strength, as elastic joint deformations reduce the rate of dilation to a value less than the asperity angle.

On the basis of the energy method considerations, and the experimental validation for regular triangular asperities, it is concluded that Ladanyi and Archambault's expression for global shear stress based on the joint dilation rate as given by Eq. (10) is incorrect for rock joints in which high asperity contact stresses result in significant local elastic deformations. In order to estimate the reduction effect of these elastic deformations on the rate of dilation, local contact stresses must be estimated. As these are critically dependent on global stress, joint geometry and shear displacement, no general guidelines can be given. However, the authors have successfully combined a probabilistic approach for roughness characterization (Seidel and Haberfield, 1995) with a mechanistic model of asperity behaviour (Seidel and Haberfield, 1994) to estimate the shear response of joints taking elasticity into account.

It is acknowledged that for joints in hard rock under low normal stress conditions, the effects of elasticity may be small, and the underestimate of shear strength using Ladanyi and Archambault's approach will therefore not be significant.

3. Sliding on Surfaces with Multiple Asperities of Varying Angle

The original analysis of Ladanyi and Archambault, and the preceding analysis of the effect of elasticity on joint shear stress were restricted to joints with constant asperity angles. In the case of a joint profile comprising a number of *rigid* asperities of varying asperity angle, asperity sliding can only occur on asperities with a slope angle equal to the currently steepest, or critical slope. (Initially, this will be the steepest slope angle of the profile, but subsequent asperity failures may make

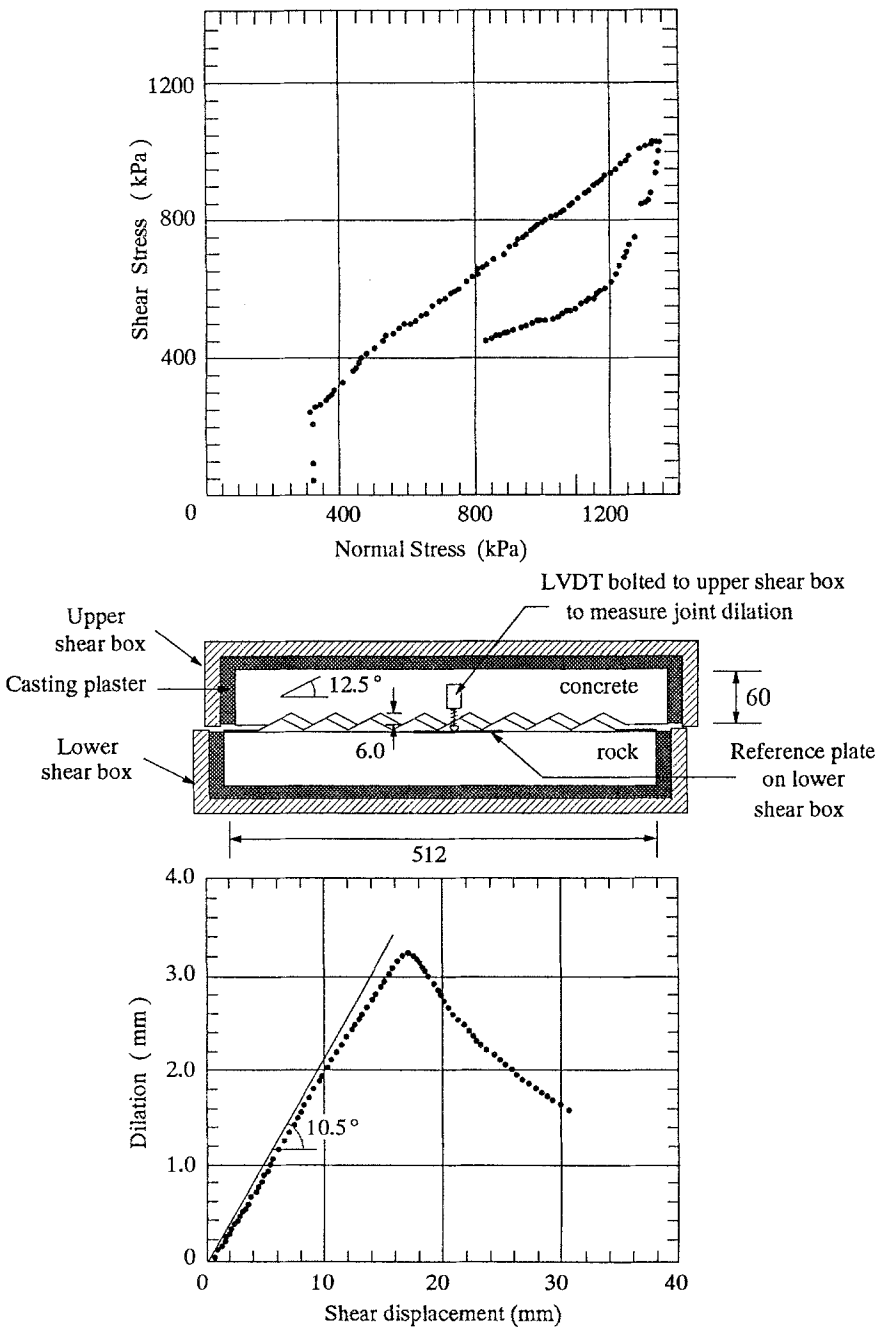

Fig. 4. Shear displacement-dilation response and stress path plot for 12.5° regular triangular asperity joint in Johnstone

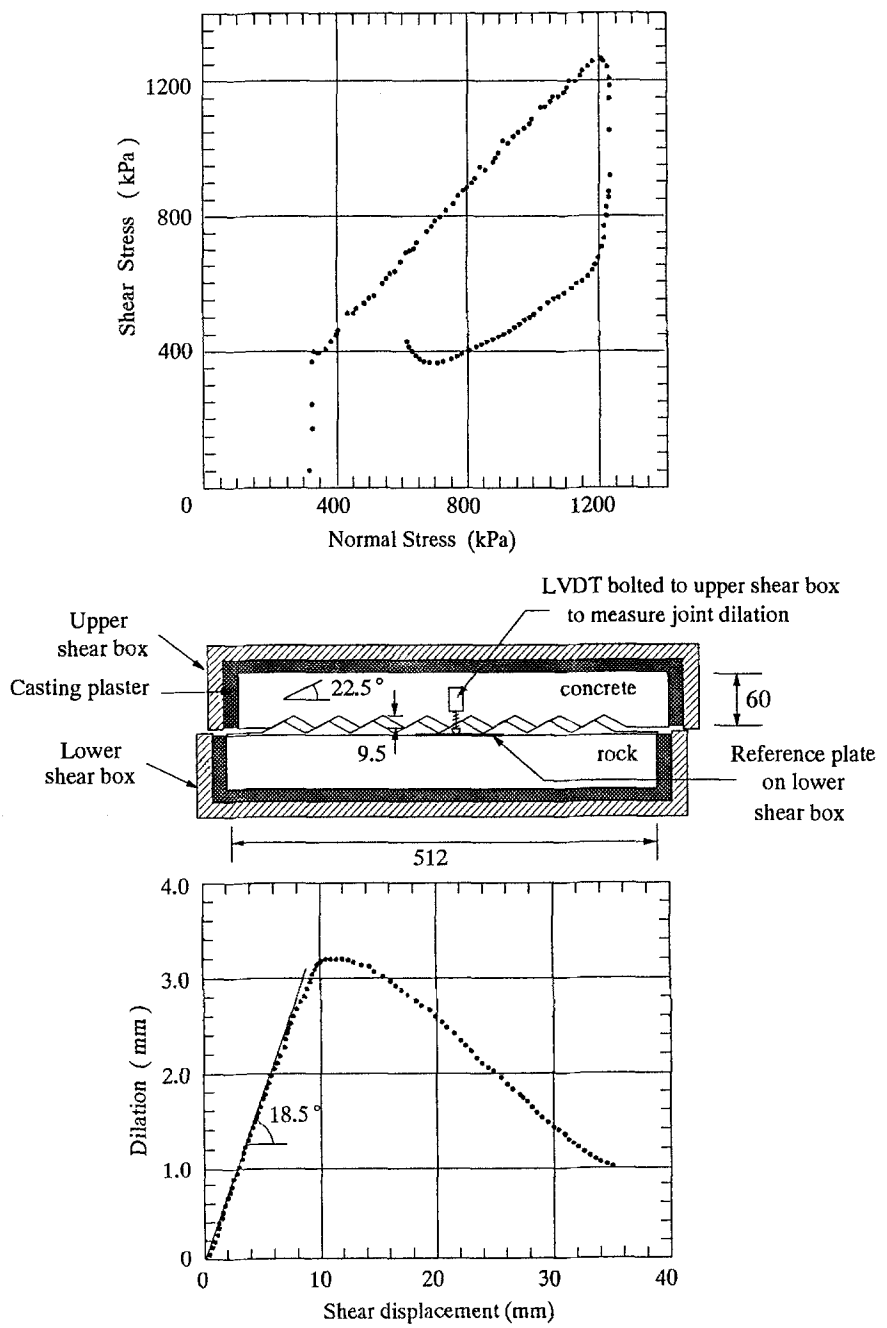

Fig. 5. Shear displacement-dilation response and stress path plot for 22.5° regular triangular asperity joint in Johnstone

Table 1. Comparison of direct shear tests and predicted effective friction angles for Johnstone

Asperity angle, i (deg)	Measured dilation angle, ν (deg)	Basic friction angle, ϕ_u (deg)	$\tan^{-1}(\tau/\sigma_n)$ from shear tests (deg)	Eqn. (12) $(\phi_u + i)$ (deg)	Eqn (10) $(\phi_u + \nu)$ (deg)
5.0	4.0	24.5	29.0	29.5	28.5
10.0	8.5	24.5	34.0	34.5	33.0
12.5	10.5	24.5	36.5	37.0	35.0
15.0	12.5	24.5	39.0	39.5	37.0
17.5	14.5	24.5	42.0	42.0	39.0
22.5	18.5	24.5	47.0	47.0	43.0
27.5	21.0	24.5	52.5	52.0	45.5

progressively shallower asperity slopes the critical slope). Any asperities with lower slope angles than the current critical slope (which we shall call subcritical) cannot be in contact, and therefore will not be involved in the sliding process.

By contrast, for joint profiles comprising *elastic* asperities, it is possible that as a result of elastic deformations of the asperities, sliding will occur both on the currently critical asperity slope and simultaneously on asperity slopes less steep than the critical slope, i.e. *sub-critical* asperity slopes (Seidel, 1993). Figure 6

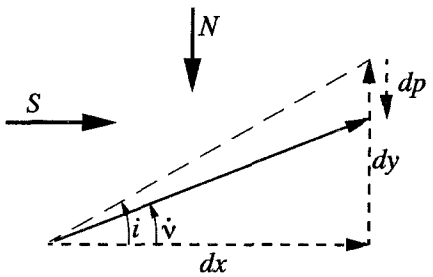

$$S_1 = \frac{N(dy-dp)}{dx} + \frac{Ndp}{dx} = N\tan i$$

$$S_2 = S\dot{\nu}\tan\phi_u$$

$$S_3 = N\tan\phi_u$$

$$S = S_1 + S_2 + S_3$$

Fig. 6. Deformations due to inelasticity

schematically represents the relevant movements for this case – a general asperity slope, i, and a critical slope, $i_c > i$, have been adopted.

It is evident that dilation at an angle larger than the sub-critical asperity angle, i, will result in an additional component, dr, of dilation against the normal force on the asperity, than would apply if the asperity were the critical asperity. However, the energy for this additional amount of dilation is provided by the release of elastic strain energy in the asperity, as long as contact is maintained. The net effect, therefore, is that the component S_1 in the energy balance remains unchanged at $N\tan i$, and not $N\tan i_c$. As discussed in the previous section, the components S_2 and S_3, being frictional, are dependent on the *relative* movements across the interface. They are unaffected by the body movement dr of the asperity and therefore remain identical to the rigid asperity components for an asperity slope of i as given by Ladanyi and Archambault.

The shear stress for each sub-critical asperity is therefore dependent only on the

basic friction angle and the angle of that asperity, and not on the overall joint dilation rate, i.e.

$$\tau = \sigma_n \tan(\phi_u + i). \tag{13}$$

From Eq. (13), the *instantaneous* shear strength of a joint of n asperities with slopes, i_j, in an elastic rock can be determined as follows:

$$\tau = \frac{1}{A} \sum_{j=1}^{j=n} a_j \sigma_{n,j} \tan(\phi_u + i_j), \tag{14}$$

where A is the total joint contact area and $\sigma_{n,j}$ are the local contact stresses which act upon the individual asperity contact areas, a_j. The *instantaneous* shear strength in this context is taken to mean the shear strength at any instant of the shear process or for any value of shear displacement; it is not simply the peak joint shear strength. For asperities which are not in contact, the relevant $\sigma_{n,j}$ term in Eq. (14) is zero, and these asperities obviously do not then contribute to the joint shear strength.

The instantaneous sliding resistance of a joint is therefore determined as the sum of individual asperity sliding resistances, which are a function only of the current asperity normal stress and the asperity angle. The sliding shear stress is dependent on the distribution of normal stresses on asperities within the joint, and the angles of those asperities as given in Eq. (14). By contrast, it is incorrect to determine the shear stress from the global normal stress and the global joint dilation rate as proposed in Eq. (10).

The spatial distribution of asperity angles in a joint can be addressed on a statistical basis, whilst the determination of the normal stresses on these asperities requires the interactions of elastic deformation due to individual asperity loading to be modelled. In an elastic rock joint with complex interface geometry, the highest stresses will be applied to the steepest asperities, with the more shallow asperities subjected to lower or even no normal stress due to lift-off. The successful application of these approaches to the prediction of complex joint performance are described in more detail in Seidel and Haberfield (1994) and Seidel (1993).

4. The Effects of Degradation on the Friction Angle of Collapsing Materials

The previous discussions have related to rocks which behave in an essentially elastic manner until the onset of asperity failure. Not all rocks, however, can be assumed to behave elastically under the application of shear stresses. Calcarenites are such a class of rock, and must therefore be modelled differently. Calcarenites are essentially composed of angular bioclastic grains that are cemented to various degrees at isolated point contacts, forming an open structure with a high void ratio. Under the application of hydrostatic confining stresses or shear stresses, the structure can collapse, either as a result of the destruction of cementing at the point contacts, or by crushing of the individual grains. This collapse is accompanied by a reduction in volume of the calcarenite, as voids are filled by the freed grains, or their debris.

Whereas the sliding response of non-degrading rocks under applied shear can reasonably be modelled as elastic, the calcarenite samples are subjected to both elastic and inelastic deformations. The elastic deformations cause recoverable strain energy to be stored in the rock. As shown previously, these elastic deformations do not affect the measured friction angle of the rock under shear. By contrast, the inelastic deformations result in permanent and non-recoverable strains in the rock, and the energy used in causing these inelastic deformations is lost in the crushing process.

Just as the energy approach of Ladanyi and Archambault (1970) was applied previously to the shear behaviour of elastic interfaces, the same approach can be used to determine the effect of inelastic deformations on the net friction angle during sliding accompanied by degradation. The schematic representation for the case of entirely inelastic deformations is shown in Fig. 6, which is essentially identical to Fig. 3, except that the elastic body deformation, *de* is replaced by a gradational inelastic deformation, *dp*.

In this case, the reduction in work done due to dilation against the normal force is not balanced by recoverable strain energy, but rather by work required, and lost, in producing the inelastic deformations (i.e. crushing the structure of the calcarenite).

Adopting the same terminology used by Ladanyi and Archambault (1970), the component S_1, which is the component due to external work required to dilate against the normal force, N, is therefore unaffected. The component due to work done in internal friction if the sample did not change volume, S_3, is also unaffected, as the shear displacement, dx, is unchanged. However, as the amount of *relative* dilation movement is reduced due to the inelastic movements (i.e. degradation), the component S_2, is reduced. If the current dilation rate, $\dot{v} < \tan i$, the component S_2 becomes:

$$S_2 = S\dot{v} \tan \phi_u \tag{15}$$

and the total shear force,

$$S = N \tan i + S\dot{v} \tan \phi_u + N \tan \phi_u, \tag{16}$$

which can be rearranged in terms of stress as:

$$\tau = \frac{\sigma_n(\tan i + \tan \phi_u)}{(1 - \dot{v} \tan \phi_u)}, \tag{17}$$

as $\dot{v} \neq \tan i$, this expression does not reduce further. The effective friction angle for a degrading material can then be expressed as:

$$\phi_{\text{degrade}} = \tan^{-1}\left[\frac{\tan i + \tan \phi_u}{1 - \dot{v} \tan \phi_u}\right]. \tag{18}$$

It can be seen from Eq. (16) that if $\dot{v} < \tan i$, the determination of sliding shear strength on the basis of dilation rate will lead to an underestimation of the true sliding shear strength for these materials.

Just as for the case of elastic asperities, Eq. (16) has been verified experimentally by Seidel (1993) for a series of constant normal stiffness direct shear tests on regular triangular joint profiles cut in a natural calcarenite, called Gambier

Limestone (James and Bone, 1989). These tests were performed as part of the previously mentioned research project into the behaviour of concrete piles socketed into weak rock, and in this particular case to the behaviour of grouted-insert piles or driven-and-grouted piles in calcareous offshores deposits; the joint in these tests therefore comprised a calcarenite/concrete interface. Asperity angles for these tests varied from 5° to 27.5° as for the tests on Johnstone, and typical interface geometry and stress-path plots are shown for tests on regular triangular calcareous asperities of 12.5° and 22.5° in Figs. 7 and 8.

The effective friction angle given in Eq. (18) for the series of tests, is compared in Table 2 with both $\tan^{-1}(\tau/\sigma_n)$ measured in the tests and the effective friction angle, $(\phi_u + i)$, suggested by Eq. (10). As the degradation rate changes with the applied normal stress, all comparisons in Table 2 are based on analysis of the responses at peak shear strength. It is clear from this table that the observed joint sliding friction angle, $[\tan^{-1}(\tau/\sigma_n)]$ is most closely predicted by Eq. (18). The sliding friction angle based on the asperity angle, i, (Eq. 12) consistently over-predicts the measured friction angle; conversely, Eq. (10), based on the observed dilation rate, underpredicts the measured friction angle.

As noted previously, Eq. (18) is based on deformations at the interface of the degrading material being entirely inelastic. In practice, deformations will comprise both inelastic and elastic components. This would account for the differences between Eq. (18) and the observed friction angle. Furthermore, in order to predict the joint response in degrading materials, the elastic and inelastic components must be computed individually and treated separately. It is important, therefore, to be able to predict the instantaneous rate of degradation.

On the basis of the energy method considerations, and the experimental results for regular triangular asperities in calcarenite, it is concluded that Ladanyi and Archambault's expression for global shear stress based on the joint dilation rate as given by Eq. (10) is incorrect for rock joints which undergo inelastic deformations. For such rocks, Eq. (10) *must* underestimate the joint shear strength; Equation (17) will more correctly predict joint shear strength.

As for the elastic asperity case described previously, the shear resistance of multi-asperity profiles in degrading rocks, and with varying asperity angles is computed by combining the individual shear resistance of each individual asperity face as follows:

$$\tau = \frac{1}{A}\sum_{j=1}^{j=n} a_j \sigma_{n,j} \frac{(\tan\phi_u + \tan i_j)}{(1 - \dot{\nu}\tan\phi_u)}. \tag{19}$$

5. Conclusions

According to Ladanyi and Archambault, joint shear strength of natural joints can be determined from the applied normal stress, the basic friction angle of the rock and the joint dilation rate [see Eq. (10)]. The authors have investigated the performance of concrete-rock joints as part of an extensive research program

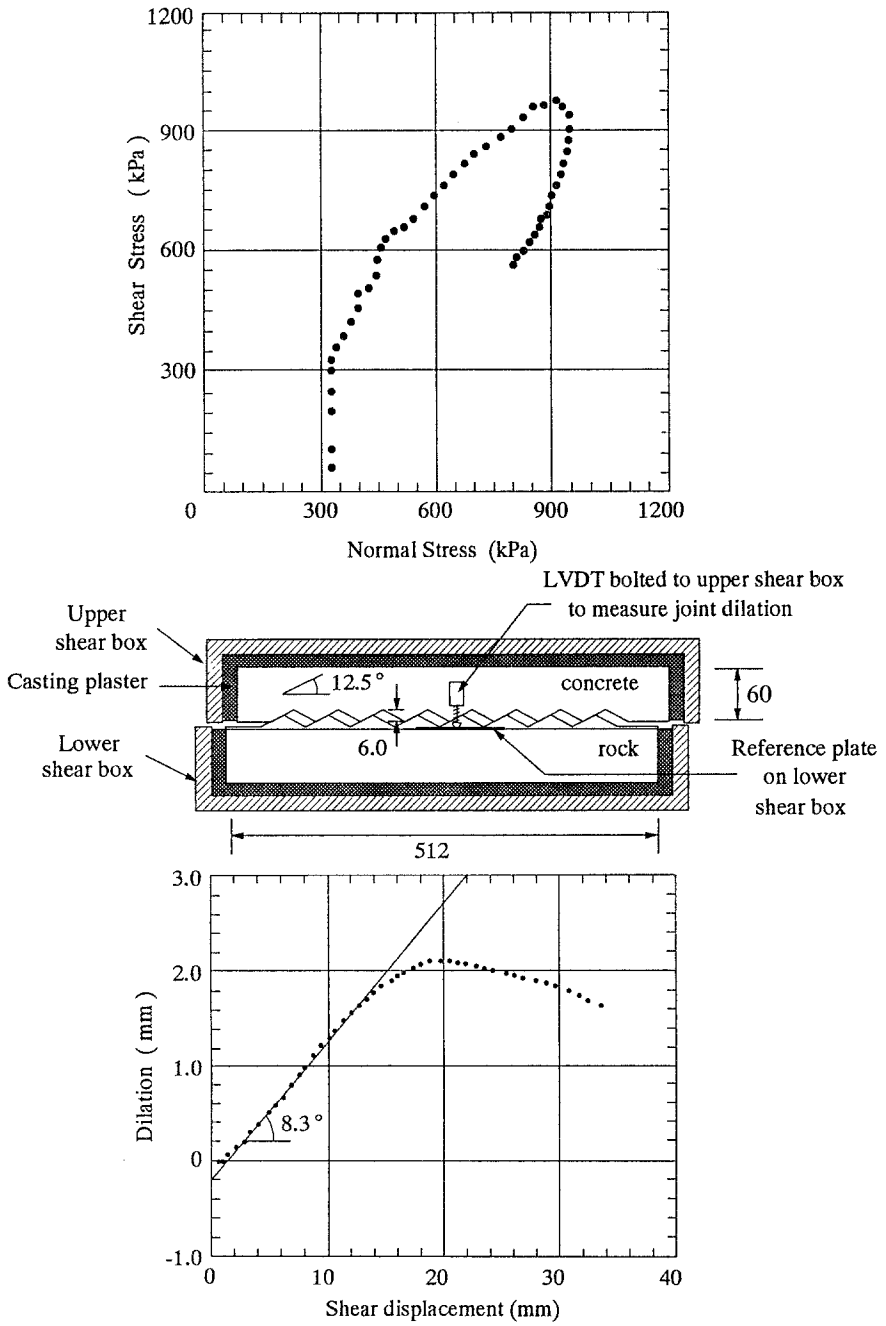

Fig. 7. Shear displacement-dilation curve and stress path plot for 12.5° regular triangular asperity joint in Calcarenite

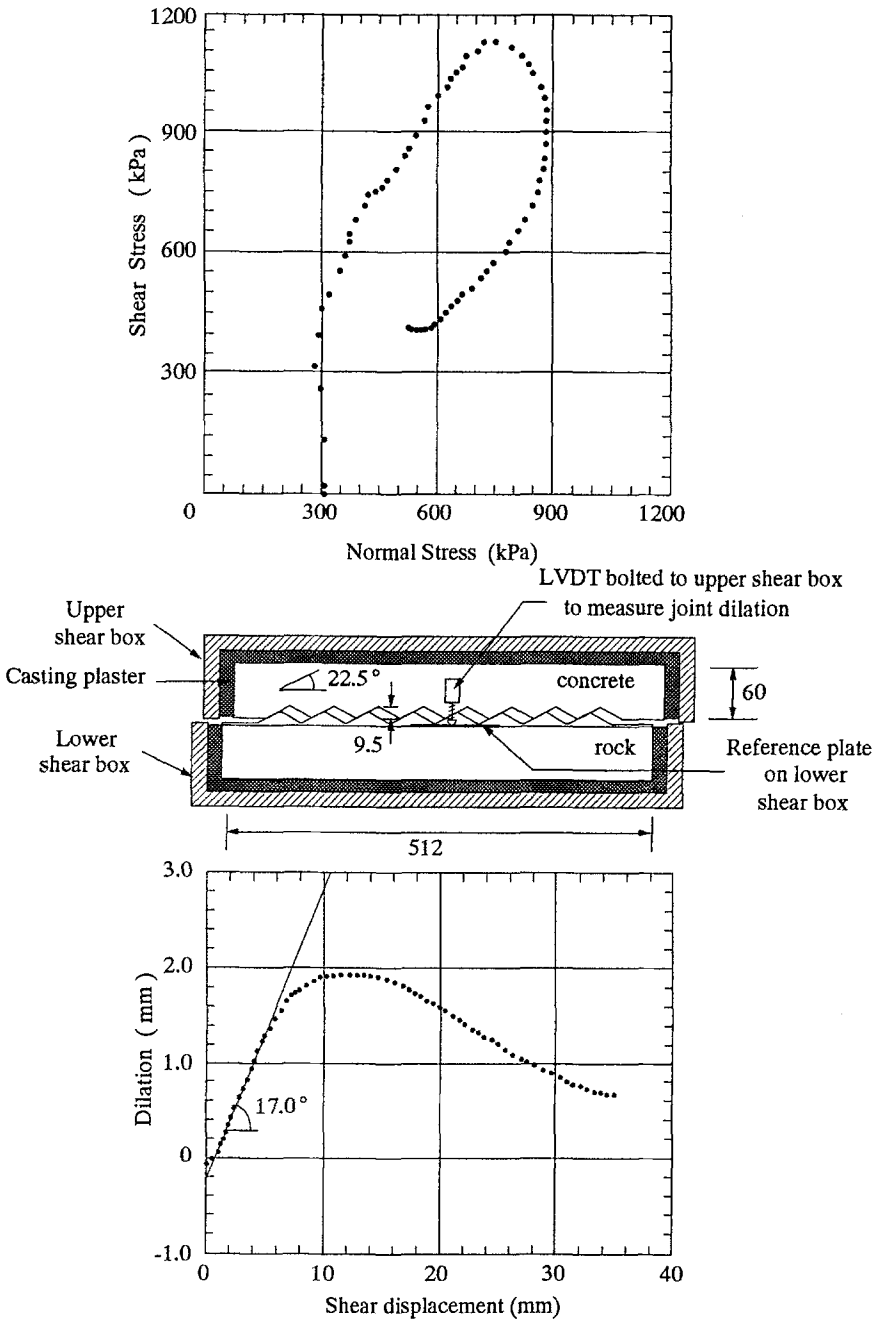

Fig. 8. Shear displacement-dilation curve and stress path plot for 22.5° regular triangular asperity joint in Calcarenite

Table 2. Comparison of direct shear tests and predicted effective friction angles for Calcarenite at peak shear

Asperity angle, i (deg)	Measured dilation angle, ν (deg)	Basic friction angle, ϕ_u (deg)	$\tan^{-1}(\tau/\sigma_n)$ from shear tests (deg)	Eqn. (18) ϕ_{degrade} (deg)	Eqn. (12) $(\phi_u + i)$ (deg)	Eqn. (10) $(\phi_u + \nu)$ (deg)
5.0	1.2	37.5	42.1	41.0	42.5	38.7
10.0	2.9	37.5	44.5	44.5	47.5	40.4
12.5	3.8	37.5	47.0	46.2	50.0	41.3
17.5	10.5	37.5	51.3	49.7	55.0	48.0
22.5	11.9	37.5	56.1	54.7	60.0	49.4
27.5	14.4	37.5	60.0	58.1	65.0	51.9

into the behaviour of piles socketed into weak rock. As part of this research, it has been shown by applying conservation of energy principles, that for natural rocks, the assumption of rigidity made by Ladanyi and Archambault in their model, leads to an underestimate of the available sliding friction strength. By contrast, the joint shear strength of elastic rocks is dependent not on the dilation rate, but on the individual asperity angles and the distribution of normal stresses on those asperities.

The conservation of energy principles have also been used to determine the shear strength of asperities of degrading materials, such as calcarenite. It has been shown in all cases that the use of dilation angle as proposed by Ladanyi and Archambault will underestimate joint shear strength. The theoretical derivations have in all cases been substantiated experimentally.

The sliding models developed in this paper have been used in a new analytical model for the prediction of the shaft resistance of concrete piles socketed into rock (Seidel and Haberfield, 1994). The principles, however, can be applied to the more general case of natural rock joints.

6. Acknowledgments

The authors acknowledge the assistance of both the Australian Research Council and the Sir James McNeill Foundation in funding the work described in this paper.

References

Haberfield, C. M., Johnston, I. W. (1994): A mechanically-based model for rough rock joints. J. Rock Mech. Min. Sci. Geomech. Abstr. 31.

James, N. P., Bone, Y. (1989): Petrogenesis of Cenozoic, temperate water calcarenites, South Australia: a model for meteoric/shallow burial diagenesis of shallow water calcite sediments. J. Sedimentary Petrol. 59 (2), 191–203.

Johnston, I. W., Choi, S. K. (1986): A synthetic soft rock for laboratory model studies. Géotechnique 36(2), 251–263.

Ladanyi B., Archambault, G. (1970): Simulation of shear behaviour of a jointed rock mass. In: Proc., 11th Symp. on Rock Mechanics: Theory and Practice, AIME, New York, 105–125.

Patton, F. D. (1966): Multiple modes of shear failure in rock. In: Proc, 1st Cong. Int. Soc. Rock Mech. Lisbon, 509–513.

Rowe, P. W. (1962): The stress dilatancy relation for static equilibrium of an assembly of particles in contact. In: Proc., Royal Soc. A. 269, 500–527.

Rowe, P. W., Barden, L., Lee, I. K. (1964): Energy components during the triaxial cell and direct shear tests. Géotechnique 14, 247–261.

Seidel, J. P. (1993): The analysis and design of pile shafts in weak rock. PhD Dissertation, Monash University, Dept. Civil Engineering, Clayton, Australia.

Seidel, J. P., Haberfield, C. M. (1994): A new approach to the prediction of drilled pier performance in rock. In: Proc., FHWA Int. Conf. on Design and Construction of Deep Foundations, Orlando Vol. 2, 556–570.

Seidel, J. P., Haberfield, C. M. (1995): Towards an understanding of joint roughness. Rock Mech. Rock Engng. 28(2), 69–92.

Authors' address: Dr Julian Seidel, Monash University, Department of Civil Engineering, Clayton, Victoria, 3168 Australia.